

Efficient sampling in complex materials at finite temperature: the thermodynamically-weighted activation-relaxation technique

Normand Mousseau*

*Département de Physique, Université de Montréal, C.P. 6128,
Succursale Centre-ville Montréal, Québec, Canada H3C 3J7.*

G.T. Barkema†

*Institute for Theoretical Physics, Utrecht University,
Leuvenlaan 4, 3584 CE Utrecht, the Netherlands*

(Dated: February 7, 2020)

We present an accelerated algorithm that samples correctly the thermodynamic ensemble in complex systems where the dynamics is controlled by activation barriers. The efficiency of the thermodynamically-weighted activation-relaxation technique (THWART) is many orders of magnitude greater than standard molecular dynamics, even at room temperature and above, in systems as complex as proteins and amorphous silicon.

PACS numbers: 5.10.-a, 5.70.-a, 66.30.-h, 82.20.Wt

Throughout physics, chemistry and biology, a large proportion of atomistic processes take place on time scales many orders of magnitude longer than the typical phonon period. These processes are out of reach of single time-scale algorithms, such as molecular dynamics (MD), which can reach simulation times equivalent to the microsecond at best. In view of this limitation, considerable effort has been devoted in the last few years to develop algorithms that allow spanning multiple time scales. These algorithms include the activation-relaxation technique (ART) [1, 2] and similar techniques [3, 4] which sample the configurational landscape by identifying transition paths from minimum to minimum, as well as accelerated schemes based on molecular dynamics such as hyper-MD [5], temperature-assisted dynamics [6] and others [7].

ART and similar methods have been applied with success to study the topology of the energy landscape and activated mechanisms in a wide range of materials including amorphous and crystalline semiconductors [8, 9, 10], glassy materials [11], atomic clusters [2, 12] and proteins [13, 14, 15]. ART defines events in the energy landscape as a two-step process: (1) the system is first activated from a local energy minimum to a nearby saddle-point and (2) then relaxed to a new minimum. Since the landscape constructed by ART consists only of local minima connected via saddle points, the entropic contributions to sampling are neglected so it is not possible to guarantee a proper statistical sampling, especially at elevated temperatures where the harmonic approximation breaks down.

Accelerated MD schemes, on the other hand, rely either on deforming the energy landscape [5, 7] or on some projection from high-temperature simulations [6]. In the first case, the energy basin surrounding a local minimum

is filled according to various rules. In the second case, multiple simulations are performed at high temperature and as soon as an event occurs, the time is rescaled with an appropriate factor. These methods work only for simple systems, however, where it is possible to have a detailed *a priori* knowledge of the parameters defining the landscape. As soon as a wide range of barriers come into play, such as in proteins or disordered materials, it becomes very difficult to apply the appropriate transformations in order to sample correctly and efficiently the phase space.

In this Letter, we present an algorithm that provides a proper statistical sampling of the energy landscape at a wide range of temperatures irrespective of the complexity of the landscape. Combining molecular dynamics with ART, the thermodynamically-weighted activation-relaxation technique (THWART) samples the thermodynamically relevant parts of the phase space, hopping over barriers that can be many times higher than $k_B T$.

THWART generates motion in the energy landscape, a $3N$ -dimensional hypersurface, on which the height is given by the potential energy of a configuration as a function of its $3N$ atomic coordinates, where N is the number of atoms in the system. At low temperature, a configuration typically spends most of its time oscillating thermally around a local minimum, hopping over an energy barrier only when a thermal fluctuation transfers large amounts of energy onto a single mode. In this regime, it is possible to separate the energy landscape into two types of regions: basins and saddle regions. The *basins* are regions around local-energy minima where all Hessian eigenvalues, corresponding to the curvature of the landscape, are above a threshold value λ_0 . The *saddle regions* have at least one direction with a curvature (eigenvalue of the Hessian matrix) below this threshold value. These regions surround metastable points such as first or higher-order saddle points. A two-dimensional sketch of an energy landscape, paved according to these

*Electronic address: normand.mousseau@umontreal.ca

†Electronic address: barkema@phys.uu.nl

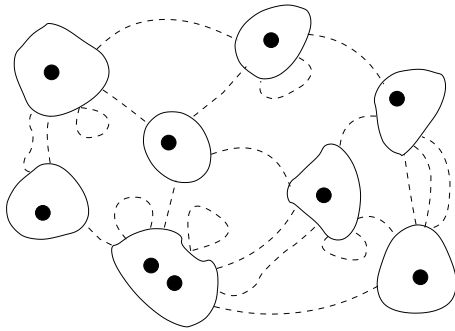


FIG. 1: Sketch of a two-dimensional energy landscape. The black dots denote the locations of local-energy minima. These minima are part of basins, bounded by a line of constant lowest-curvature (solid line); the percolating region surrounding the basins is called the saddle region. Basin-to-basin trajectories as generated by THWART are indicated by dashed lines. Constrained to ensure detailed balance, the trajectories come back to where they started if they fail to find a boundary.

criteria, is shown in Fig. 1.

At low temperature, the equilibrium properties of a system are determined by the basins, where the Boltzmann weight $\exp(-E/k_B T)$ is large and most of the sampling takes place. The partition function, $Z = \int d\vec{X} \exp(-E(\vec{X})/k_B T)$, is thus well approximated by integrating only over the basins. The basins, however, are disconnected regions in phase space and a proper sampling requires integrating over many of these basins. To ensure efficient sampling, it is therefore essential to accelerate the rate at which basins are visited.

THWART achieves this acceleration in two steps. In the basin regions, configurations are evolved using standard MD. We select the NVT ensemble and use the velocity Verlet algorithm for the integration. During the MD simulation, we monitor the lowest eigenvalue of the Hessian which defines the position of the boundary separating the basin from the saddle region. As soon as this lowest eigenvalue reaches a given threshold λ_0 , the MD is suspended and the hopping phase starts. The atomic positions at the basin boundary is identified by \vec{x}_0 and the velocities by \vec{v}_0 .

From \vec{x}_0 , on the basin boundary, we construct a fully reversible path that leads to a new basin, crossing an energy barrier. For this, we follow the eigendirection corresponding to the lowest eigenvalue away from the basin until the eigenvalue crosses the threshold λ_0 from below. In order to ensure detailed balance, the trajectory into the saddle region is further constrained to move on a hyperplane with constant potential energy. Specifically, the activated trajectory is generated by iterating the following equation:

$$\vec{x}_{i+1} = \vec{x}_i + \frac{\Delta t}{2} (\vec{h}_i + \vec{h}_{i+1}) + c (\vec{F}_{\perp,i} + \vec{F}_{\perp,i+1}). \quad (1)$$

Here, \vec{h}_i is the normalized eigenvector at \vec{x}_i correspond-

ing to the lowest (most negative) Hessian eigenvalue, $\vec{F}_{\perp,i}$ is the component of the force at \vec{x}_i perpendicular to \vec{h}_i , Δt is a constant factor that determines the size of the increment, and c is a multiplicative constant, chosen to project the trajectory onto the hyperplane of constant potential energy. The orientation of \vec{h}_0 is chosen initially so that it points towards the direction of more negative curvature, i.e., away from the initial basin; it is updated at each step by requiring that the inner product of the local eigenvector \vec{h}_i with that at the previous step, \vec{h}_{i-1} be always positive.

The move along the eigendirection corresponding to the lowest eigenvalue changes the total configurational energy. The last term on the right-hand side of Eq. (1) corrects for this change and constrains the trajectory to the hyperplane with constant energy. Because the initial configuration is thermalized, its configurational energy is well above that of the local minimum, with roughly $k_B T/2$ of additional potential energy per degree of freedom. By transferring energy to a specific degree of freedom from the heat bath formed by all the other $3N - 1$ degrees of freedom, the algorithm reproduces therefore the statistical mechanism responsible for crossing barriers. Simply moving along the force, to enforce this constraint tends to bring the configuration back to its original position. Instead, we correct the energy by moving in the reduced space generated by the hyperplane perpendicular to this eigendirection, projecting the force onto this hyperplane, $\vec{F}_{\perp,i}$.

Eq. (1) is iterated until the lowest eigenvalue passes the threshold (from below, this time) and the configuration reaches the boundary of a basin with position \vec{x}_p . At this point, the activation phase is stopped and the MD is resumed with the new positions and velocities $\vec{v}_p = \vec{v}_0$.

The path generated from \vec{x}_0 to \vec{x}_p is fully reversible: a configuration in basin p reaching \vec{x}_p would trigger the activation, bringing it to the other end of this path, in \vec{x}_0 . Reversibility is ensured by the symmetric criterion for entering and leaving the saddle region as well as by keeping the path on a hyperplane of constant energy. Reversibility is not sufficient for detailed balance, however. In continuous space, it is also necessary to verify that an infinitesimal volume surrounding \vec{x}_0 remains constant as the configuration moves along the path leading to \vec{x}_p . This transformation, given by the Jacobian, determines the change in phase space, or entropy, between these two points. We have verified numerically that the Jacobian of transformation is unity along the whole path from one basin boundary to the other. In combination with reversibility, the preservation of phase space ensures that detailed balance is respected.

We also note that the path does not always lead to a new basin. In our simulations, it is not rare to see the trajectory form a circular path, coming back exactly at the initial point, \vec{x}_0 , on the boundary after a long excursion in the saddle region. If the path does not close on itself, it generally connects to a different basin.

Having established the validity of the algorithm, we

apply THWART to two non-trivial systems: amorphous silicon and a small peptide. Simulations on amorphous silicon are performed on models with two different sizes and initial configurations. The 1000-atom model was generated with ART nouveau [2] using a modified Stillinger-Weber (mSW) potential fitted to the amorphous phase [16]. This configuration is well-relaxed and is described in Ref. [17]. The 500-atom model was produced with a bond-switching algorithm [18, 19] and simply relaxed with the mSW potential, showing higher strain than the 1000-atom model.

Both models were then evolved with MD in the standard NVT ensemble at a temperature of 600 K and 800 K, i.e., well below the melting transition temperature of ~ 2000 K for this potential, but near the crystallization temperature from the amorphous phase. The MD simulations are integrated with time steps of 1 fs and run over a simulated time of 10 ns, except for the 500-atom configuration at 800 K, which is run for 20 ns. Figs. 2 and 3 show the total squared displacement, $\langle r^2 \rangle$, between the initial configuration (which is energy-minimized) and the quenched configuration at time t , measured in the number of force evaluations (with 1 force evaluation per time step), for these four distinct runs.

For the well-relaxed 1000-atom model at 600 K, the figure shows that after a few initial local rearrangements, the MD runs remain trapped around a few nearby minima for more than 9 ns. We find a similar situation for the 800 K simulation, with the configuration diffusing slightly further but still failing to explore more than a few nearby basins during the 10 ns simulation.

The situation is quite different with THWART: In the basin, we follow the same MD procedure as above, while computing the lowest eigenvalue every 50 steps using a 20-level Lanczos scheme. The MD run is continued until this lowest eigenvalue falls below the threshold value λ_0 . To avoid moving back and forth along the same path, the MD procedure is required to take at least 400 steps. From this point, we apply Eq. (1) until the lowest eigenvalue increases above the same threshold. The total squared displacement measured as a function of the number of force evaluations for THWART is also plotted in Figs. 2 and 3; 10 million force evaluations correspond roughly to 5000 events. As can be seen, THWART explores the energy landscape many orders of magnitude faster than MD at the same temperature. THWART is slightly slower at short times, because it performs one event at a time, while MD can activate multiples events in parallel across the model. However, it rapidly surpasses MD. In particular, THWART does not seem to become trapped either at 600 K or 800 K. It is to be expected, however, that at high temperatures, when the number of events occurring in parallel starts proliferating, MD will become more efficient than THWART. From our simulations, this should happen close to the melting point.

The efficiency of THWART depends on the value of the threshold, the sole parameter in THWART. Its value impacts the ratio of basin to saddle regions on the energy

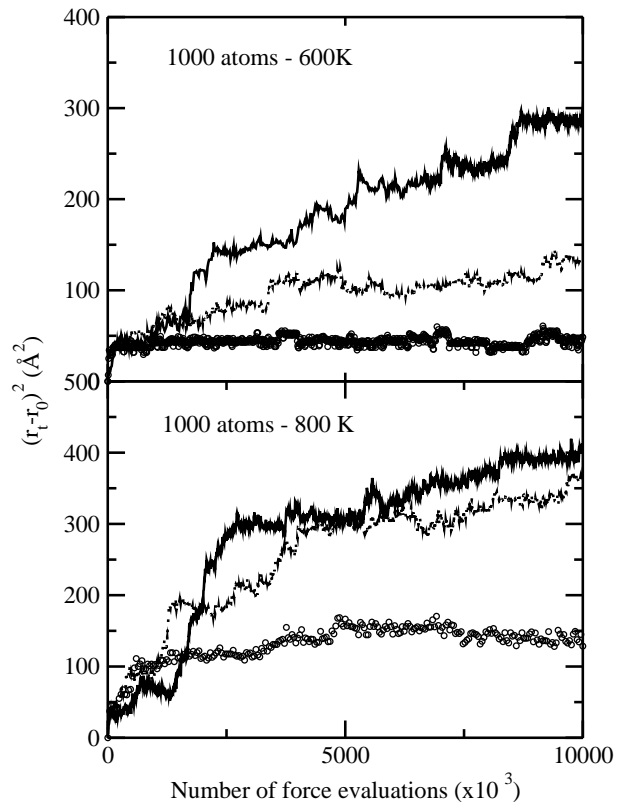


FIG. 2: Total squared displacement as a function of the number of force evaluations, at temperatures 600 K (upper box) and 800 K (lower box), obtained with MD (circles) and THWART simulations (lines). For the THWART simulations at 600 K, we use $\lambda_0 = -5\text{\AA}^2$ (solid line) and -15\AA^2 (dotted line). At 800 K, we use $\lambda_0 = -5\text{\AA}^2$ (solid line) and -10\AA^2 (dotted line).

landscape; a very low value of λ_0 reduces THWART to MD, while a high value makes THWART more similar to ART. The impact of the threshold is shown in Fig. 2, which plots the total squared displacement as a function of force evaluation for two values of λ_0 at 600 K and 800 K. At both temperatures, THWART diffuses faster with a higher threshold, which reduces the basin size but also delivers a higher fraction of open paths.

Even though the 500-atom model is more strained than the 1000-atom one, the configuration gets trapped very rapidly at 600 K with MD, within less than 1 ns. At 800 K, however, the configuration is able to overcome many barriers and diffuse significantly, becoming trapped only after about 10 ns of simulation (see Fig. 3). In spite of this considerable collective relaxation, THWART overcomes MD at 800 K, demonstrating the general efficiency of the method.

Results on a small 10-residue peptide show that THWART is also more efficient than MD for this system. We use an artificial peptide of sequence AAAAAAGAAAA with interactions described by CHARMM19 [20] and an ASP solvation term [21] as implemented by Ponder in his program Tinker [22]. The peptide is first relaxed near its

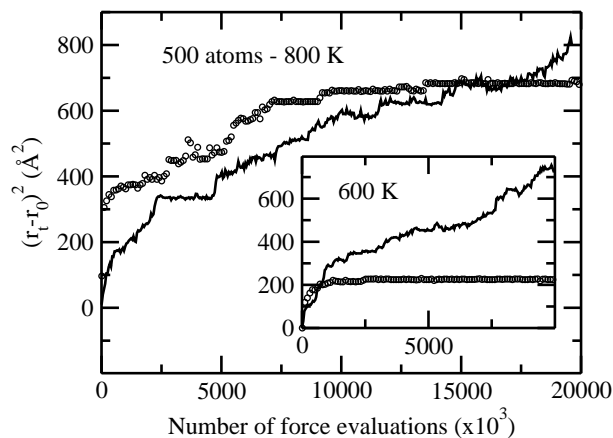


FIG. 3: Squared displacement as a function of the number of force evaluations, at a temperature of 800 K, obtained with MD (circles) and THWART simulations (lines) with $\lambda_0 = -20\text{\AA}^2$. The inset shows the same at 600 K, and with $\lambda_0 = -5\text{\AA}^2$.

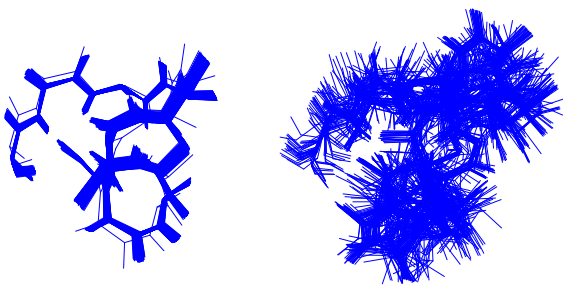


FIG. 4: Superimposed energy-minimized backbone configurations of the peptide at different times, in MD (left) and THWART (right) simulations at a temperature of 600K. About 100 configurations are superimposed for each method.

energy minimum using THWART. This sequence possesses a large number of metastable minima surrounding this lowest-energy state.

We first perform a 300-ps constant-temperature MD simulation using Tinker. To characterize the efficiency of sampling, the energy-minimized conformations after every 2 ps are graphically superimposed in the left panel of Fig. 4. Clearly, the conformation is trapped in a few nearby local minima. Next, a THWART simulation is performed of the same system over 300 000 force evaluations, or about 150 events. The energy-minimized conformations are superimposed in the right panel of Fig. 4. THWART clearly samples the phase space around the initial state much more efficiently than MD.

In summary, the thermodynamically-weighted activation-relaxation technique is an accelerated algorithm for sampling efficiently the relevant parts of the phase space in systems where the dynamics is controlled by activation barriers. THWART samples correctly the thermodynamic ensemble, with an efficiency many orders of magnitude greater than standard molecular dynamics, even at room temperature and above. We have shown that THWART is efficient in various complex systems such as proteins and amorphous silicon. THWART should be particularly useful to study materials such as glasses and proteins in water, where other accelerated techniques fail.

Acknowledgements. NM acknowledges support from the Natural Science and Engineering Council of Canada as well as NATEQ. NM is a Cottrell Scholar of the Research Corporation.

-
- [1] G. T. Barkema and N. Mousseau, Phys. Rev. Lett. **77**, 4358 (1996).
 - [2] R. Malek and N. Mousseau, Phys. Rev. E **62**, 7723 (2000).
 - [3] J. Doye and D. Wales, Z. Phys. D Atom. Mol. Cl. **40**, 194 (1997).
 - [4] G. Henkelman and H. Jónsson, J. Chem. Phys **111**, 7010 (1999).
 - [5] A. F. Voter, Phys. Rev. Lett. **78**, 3908 (1997).
 - [6] A. F. Voter, J. Chem. Phys. **106**, 4665 (1997).
 - [7] M. Iannuzzi, A. Laio, and M. Parrinello, Phys. Rev. Lett. **90**, 238302 (2003).
 - [8] G. T. Barkema and N. Mousseau, Phys. Rev. Lett. **81**, 1865 (1998).
 - [9] F. E. Mellouhi, N. Mousseau, and P. Ordejon, in preparation (2003).
 - [10] T. F. Middleton and D. J. Wales, Phys. Rev. B **64**, 024205 (2001).
 - [11] N. Mousseau, G. T. Barkema, and S. de Leeuw, J. Chem. Phys. **112**, 960 (2000).
 - [12] J. Doye, M. A. Miller, and D. J. Wales, J. Chem. Phys. **110**, 6896 (1999).
 - [13] N. Mousseau, P. Derreumaux, G. T. Barkema, and R. Malek, J. Mol. Graph. Mod. **19**, 78 (2001).
 - [14] P. N. Mortenson and D. J. Wales, J. Chem. Phys. **114**, 6443 (2001).
 - [15] G. Wei, N. Mousseau, and P. Derreumaux, J. Chem. Phys. **117**, 11379 (2002).
 - [16] R. L. C. Vink, G. T. Barkema, W. F. van der Weg, and N. Mousseau, J. Non-Cryst. Solids **282** (2001).
 - [17] F. Valiquette and N. Mousseau, Phys. Rev. B **in press** (2003).
 - [18] G. T. Barkema and N. Mousseau, Phys. Rev. B **62**, 4985 (2000).
 - [19] R. L. C. Vink, G. T. Barkema, M. A. Stijnman and R. H. Bisseling, Phys. Rev. B **64**, 245214 (2001).
 - [20] E. Neria, S. Fischer, and M. Karplus, J. Chem. Phys. **105**, 1902 (1996).
 - [21] D. Eisenberg and A. McLachlan, Nature **319**, 199 (1986).
 - [22] P. Ren and J. Ponder, J. Comput. Chem. **23**, 1497 (2002).